

The Wolf–Rayet nebula NGC 6888 as a pressure driven bubble

A. P. Marston and J. Meaburn *Department of Astronomy, The University, Manchester M13 9PL*

Accepted 1988 March 25. Received 1988 March 21; in original form 1988 February 11

Summary. Profiles of the H α and [NII] emission lines have been obtained across the major axis of the Wolf–Rayet ring nebula NGC 6888 with the Manchester echelle spectrometer combined with the Isaac Newton Telescope. Although triple profiles are found, this nebula is shown to approximate to a shell of radius 3 pc expanding at 85 km s⁻¹. The ionized mass in the shell is $3.5 \pm 1.2 M_{\odot}$. IRAS survey maps also reveal a shell of neutral material containing $40 M_{\odot}$, assuming the far infrared continuum emission from warm dust dominates the line emission. If it is assumed that this mass is also expanding at 85 km s⁻¹ it is shown that the nebula is a pressure driven bubble, which conserves the kinetic energy of the driving stellar wind.

1 Introduction

The ring nebula NGC 6888 (S105) centred on RA 20^h 10^m 5, Dec. 38° 12', is a shell of material apparently surrounding the WN6 star HD 192163 (Parker 1978). We have adopted a distance to NGC 6888 of 1.45 kpc (Wendker *et al.* 1975), however, this value is somewhat uncertain due to the ± 1 magnitude scatter in the M_v calibration for WN6 stars (Conti *et al.* 1983). Optical photographs, including those through interference filters (Parker 1978), indicate a non-spherical nebula with apparent dimensions of 7.6 \times 5.0 pc. The shell has been found to be over-abundant in nitrogen and helium, but no variation in nitrogen abundance across the nebula has been noted (Kwitter 1981).

The proposal that ring nebulae, such as NGC 6888, are produced by strong stellar winds sweeping up the ambient interstellar medium was first made by Johnson & Hogg (1965), an idea which has been modelled in detail by Weaver *et al.* (1977). However, the interaction may also more generally include stellar UV radiation or ejected stellar material.

Treffers & Chu (1982), in a review of ring nebulae associated with Wolf–Rayet (WR) stars, suggested that these are indeed shells driven by stellar winds but which are momentum rather than energy conserving. The origin of the material in such a shell is still a subject for discussion with three possible alternatives:

- (i) swept up red supergiant ejecta,

- (ii) swept up interstellar medium or
- (iii) shell material ejected from the WR star.

The existence of large internal motions in NGC 6888 has been well established previously by Johnson & Songsathaporn (1981), Lozinskaya (1970) and Treffers & Chu (1982) amongst others. Recent work on another WR nebula, RCW 104, has shown the presence of high speed knots of nitrogen rich material. These are thought to be either radiatively ionized stellar ejectae or mass-loaded wind driven flows around clumps in the surrounding medium (Goudis, Meaburn & Whitehead 1988; Hartquist *et al.* 1986). A search for evidence of such dynamical peculiarities, together with a study of the overall kinematics of NGC 6888 has now been made. These new spectral observations have been combined with *IRAS* survey data covering the region of NGC 6888, in the 12, 25, 60 and $100\ \mu\text{m}$ bands, to explain the origin of the nebular material.

2 Observations and results

The Manchester echelle spectrometer (Meaburn *et al.* 1984) combined with the image photon counting system (Boksenberg & Burgess 1973) was used in its primary spectroscopic mode at the $f/15$ focal station of the 2.5 m Isaac Newton Telescope on La Palma, on the nights of 1987 July 5/6–7/8. A $300\ \mu\text{m}$ wide slit was used, which is ≈ 1.65 arcsec on the sky and gives a resolution of $13\ \text{km s}^{-1}$. The slit positions over NGC 6888 are shown in Fig. 1. Six slit lengths (1–6 in Fig. 1) formed a line across the nebula along the major axis (PA= 35°) of the object with the midpoint

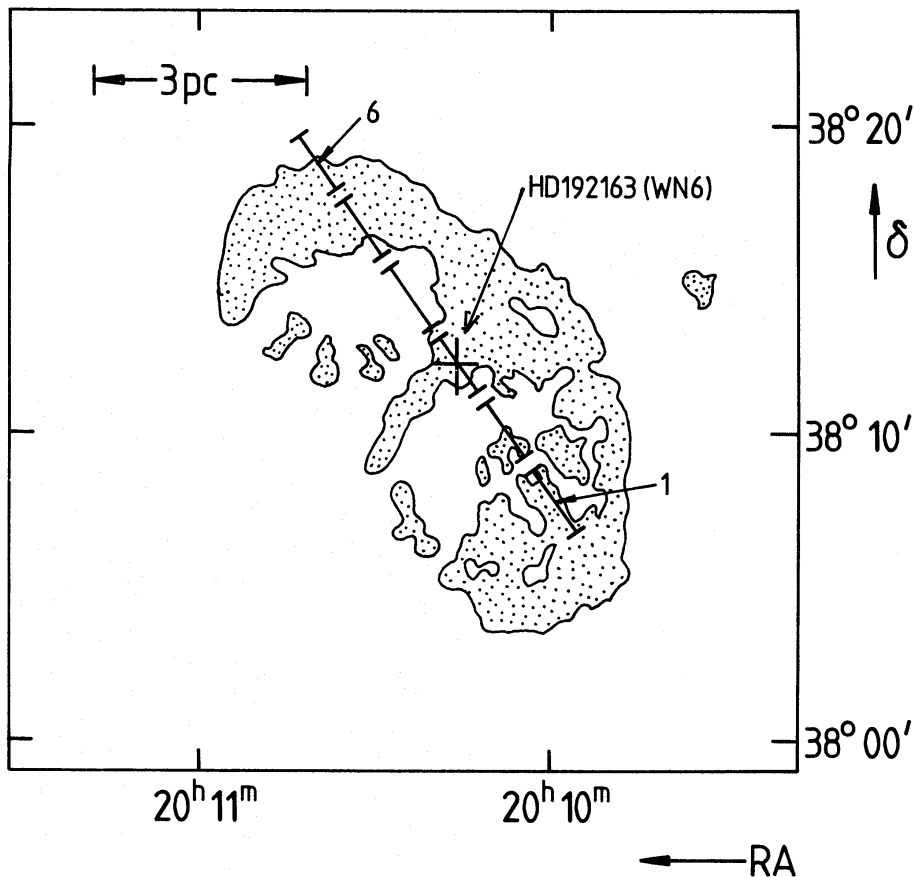


Figure 1. A sketch of the image of NGC 6888 on the Palomar *E* plate. The slit positions (1–6) along which $H\alpha$ and $[\text{N II}] 6548+6584\ \text{\AA}$ profiles were obtained are shown. The position of the central Wolf–Rayet star (HD192163) is also indicated.

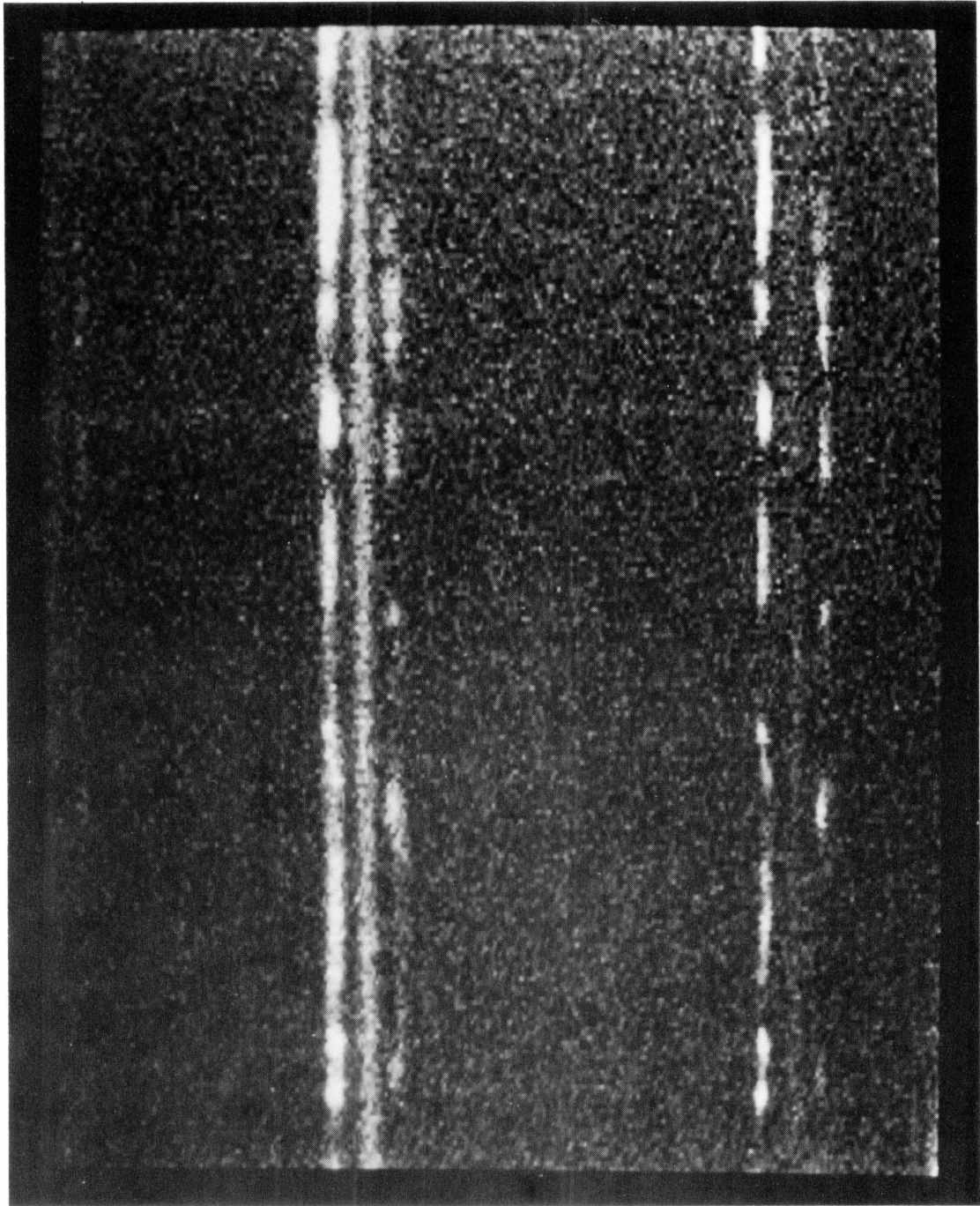


Plate 1. A grey-scale representation of the positional/velocity data for slit position 4 (Fig. 1). The triply split $H\alpha$ line is to the left with the $[\text{N II}]$ 6584 Å line similarly split to the right hand side. The north-western end of the slit is towards the top.

[facing page 392]

Table 1. Table of observations made of the NGC6888 nebula with the Manchester echelle spectrometer.

Position	Exposure (s)
3" south of WR star	1800
151" NE at PA=35°	1800
302" NE at PA=35°	1800
453" NE at PA=35°	1800
151" SW at PA=35°	1800
302" SW at PA=35°	1800

(marked 0 in Fig. 2) being placed 3 arcsec below HD192163. Each slit position produced 250 separate profiles of the $H\alpha$ and $[N\text{II}]$ 6584 and 6548 Å lines at intervals of 0.536 arcsec for a total slit length of 134 arcsec. The absolute surface brightness of the profiles were determined by obtaining a spectrum of the standard star BD+28° 4211 (Stone 1974). The variation of the $H\alpha/[N\text{II}]$ brightness ratios along the slit were also obtained.

2.1 KINEMATICS

At many positions along the slit lengths three velocity components are evident in both the $H\alpha$ and $[N\text{II}]$ profiles (an example is shown in Fig. 3 also see Plate 1). The central component of the profiles being due to galactic emission. These immediately suggest a large bubble of ionized gas,

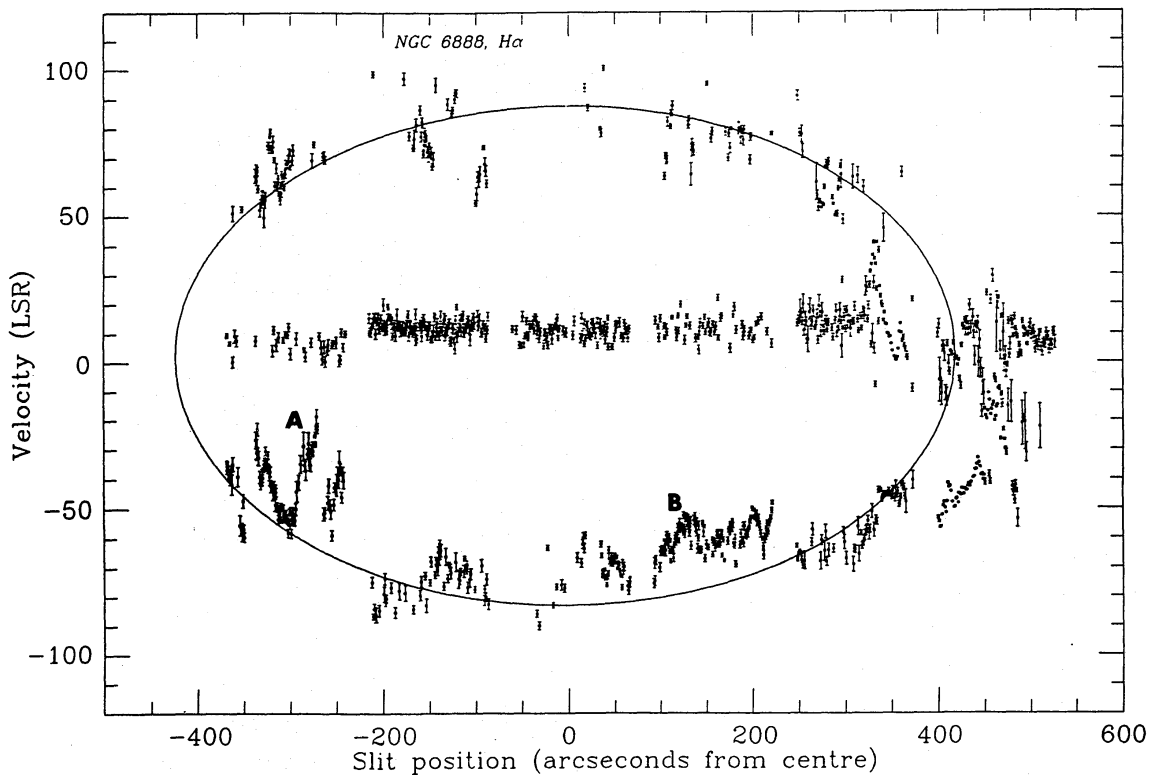


Figure 2. The overall velocity field of NGC6888 determined from Gaussian fits to the $H\alpha$ line profiles taken along the line from south-west (left) to north-east (right) marked in Fig. 1. Regions of blue-shifted material marked A and B show particularly intense emission. A velocity ellipse corresponding to a spherical shell expanding radially at 85 km s^{-1} and with a radius of 3 pc is superimposed.

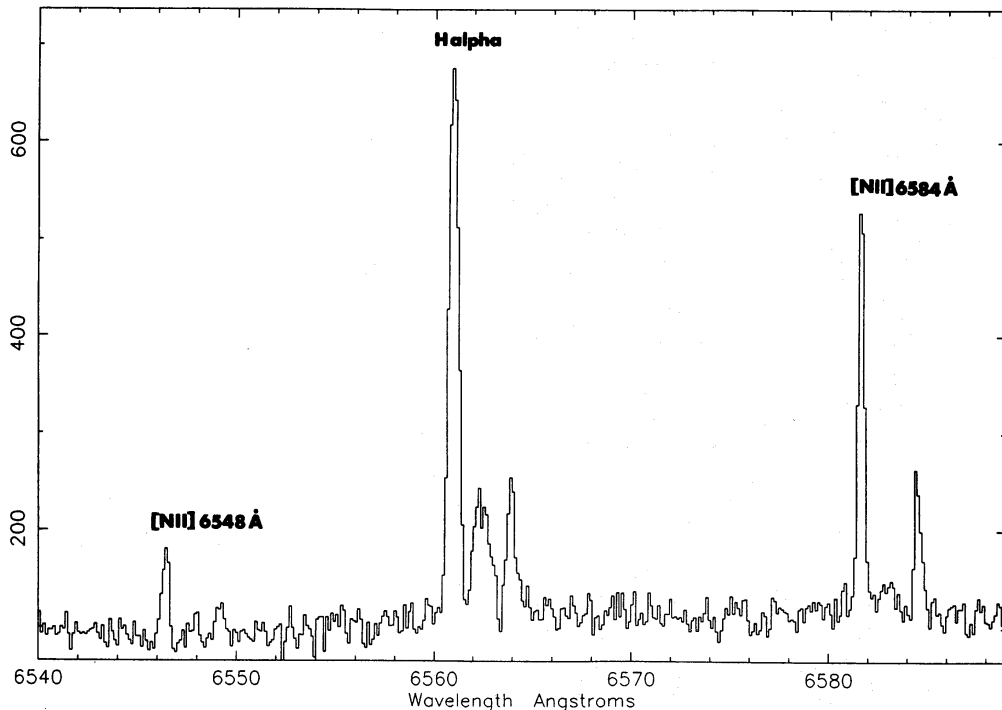


Figure 3. An example of the $H\alpha$ and $[N\text{II}]6548+6584 \text{ \AA}$ line profiles from a region with triple components at a position of $+160$ arcsec from the centre of NGC 6888, as marked on Fig. 2. The intensity scale is in IPCS counts, where 1 count $\approx 6.0 \times 10^{-6} \text{ erg cm}^{-2} \text{ s}^{-1} \text{ \AA}^{-1}$.

as previously noted by Treffers & Chu (1982) and Johnson & Songsathaporn (1981). Most emission appears to come from material blue-shifted towards us. This effect is probably real as little obscuration is apparent in the nebula (the calculated optical depth at $H\alpha$, due to dust in the shell, is $\tau_D \approx 0.017$, see later section). Regions of excess line emission are noted at the rim of the nebula and also in patches across it. Small knots (≈ 0.01 pc across) are also observed and are probably fragmentations of the shell. The full widths at half maxima (FWHM) of the $[N\text{II}]$ lines, when compared with those of $H\alpha$ suggest that the turbulent widths (convolved with thermal broadening) are larger in the $[N\text{II}]$ emitting regions. Taking the temperature of the nebula as 8000 K and the instrumental broadening as 12 km s^{-1} , the turbulent widths of the $[N\text{II}]$ and $H\alpha$ lines are then 24 and 18 km s^{-1} respectively at the centre of the nebula, decreasing to approximately 14 km s^{-1} at the edge of the shell.

The variations in V_{LSR} ($V_{\text{LSR}} = V_{\text{HEL}} + 17.7 \text{ km s}^{-1}$) of separate components in the $H\alpha$ and $[N\text{II}]$ profiles along the line of measurements over NGC 6888 are shown in Fig. 2, compared with a velocity ellipse corresponding to a bubble of ionized gas expanding radially at 85 km s^{-1} with a radius of 420 arcsec (≈ 2.95 pc). This ellipse was found to be the most reasonable eyeball fit to the data, with expansion velocities differing by $\pm 3 \text{ km s}^{-1}$ producing ellipses markedly different from the observed velocity field. A systemic velocity to the system of $+3 \text{ km s}^{-1}$ (LSR) is suggested which is approximately -10 km s^{-1} relative to the ambient component to the emission (the central component of the three). Areas of strong line emission appear to have somewhat slower expansion velocities than 85 km s^{-1} . These areas of enhanced emission have lower $H\alpha/[N\text{II}]$ ratios (see Fig. 4). No high velocity knots are seen in NGC 6888 (*cf.* RCW 104, Goudis, Meaburn & Whitehead 1988) and no evidence of non-Gaussian flow components to the profiles is observed.

Turbulent motions are most evident at the edge of the nebula (460 arcsec from the centre) where a small bubble of emission can be seen (8 arcsec across ≈ 0.06 pc). This is probably an arc of emission superimposed on the background galactic emission velocity field.

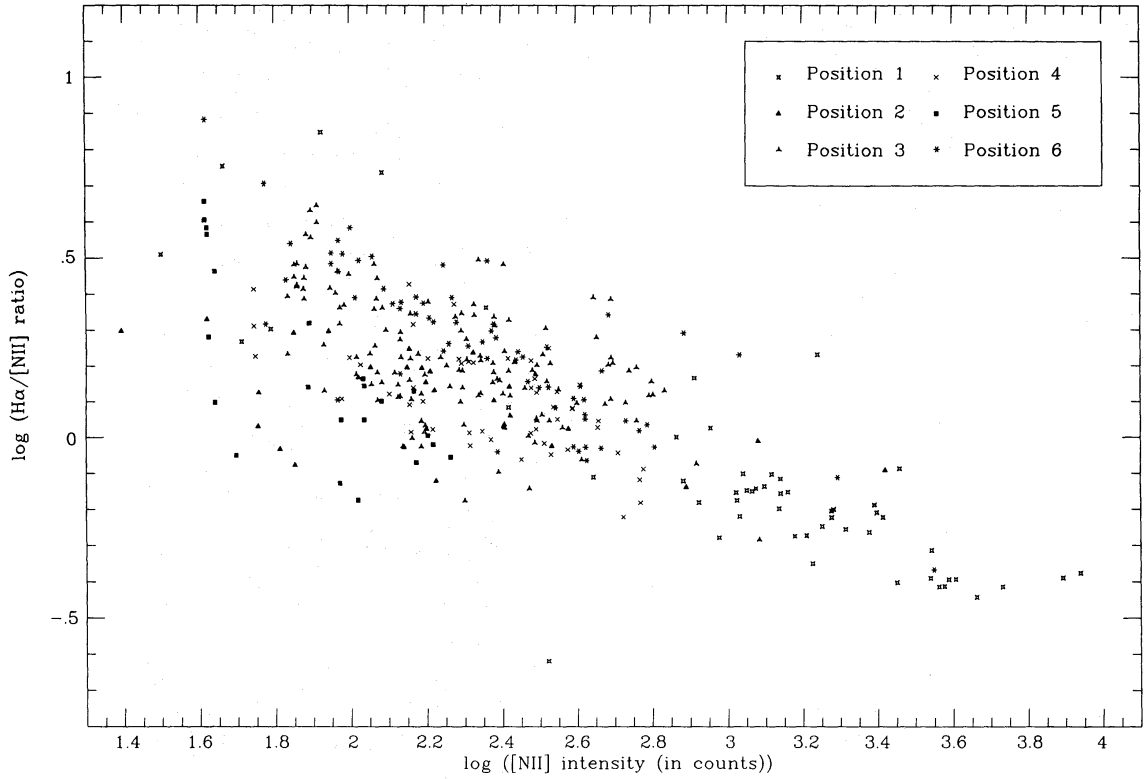


Figure 4. The correlation between the $H\alpha/[NII]$ 6584+6548 Å ratios and the $[NII]$ 6584+6548 Å intensities (in IPCS counts). The positions marked 1–6 on Fig. 1 have data points marked with different symbols, as shown in the key.

The present echelle observations are deeper than previous observations of the region and show the existence of triple components over a large area of the nebula (*cf.* Johnson & Songsathaporn 1981, and fig. 2 of Treffers & Chu 1982). More accurate kinematical and intensity information is therefore available. The bubble of material is observed to be somewhat inhomogeneous with patches of excess emission moving at velocities somewhat slower than the expansion velocity alongside smaller areas of higher velocity material. There is no evidence for the flowing cavities, put forward as a model for the region by Johnson & Songsathaporn (1981).

2.2 $H\alpha$ EMISSION

The total $H\alpha$ intensity, $I_{H\alpha}$, from NGC 6888 was estimated by integrating the average absolute $H\alpha$ brightness that was found along the slit lengths over the whole solid angle of the nebula, and was found to be

$$I_{H\alpha} = 3.0 \pm 1.0 \times 10^{-9} \text{ erg cm}^{-2} \text{ s}^{-1}. \quad (1)$$

This is equivalent to a luminosity in $H\alpha$ of $7 \pm 3 \times 10^{35} \text{ erg s}^{-1}$ at a nebular distance of 1.45 kpc. The Lyman continuum flux of photons needed to create such emission is given by Meaburn (1983),

$$S_{\text{Lyc}} = 6.8 \times 10^{49} I_{H\alpha} D^2 \text{ photon s}^{-1} \quad (2)$$

where D is the distance to the nebula in parsecs. For $D = 1.45 \text{ kpc}$ (see Section 1), the Lyman continuum flux is calculated to be $S_{\text{Lyc}} = 4.2 \times 10^{47} \text{ photon s}^{-1}$, in good agreement with Van Buren's (1986) calculated value. We can also calculate the mass, M_{HII} , of associated ionized hydrogen in

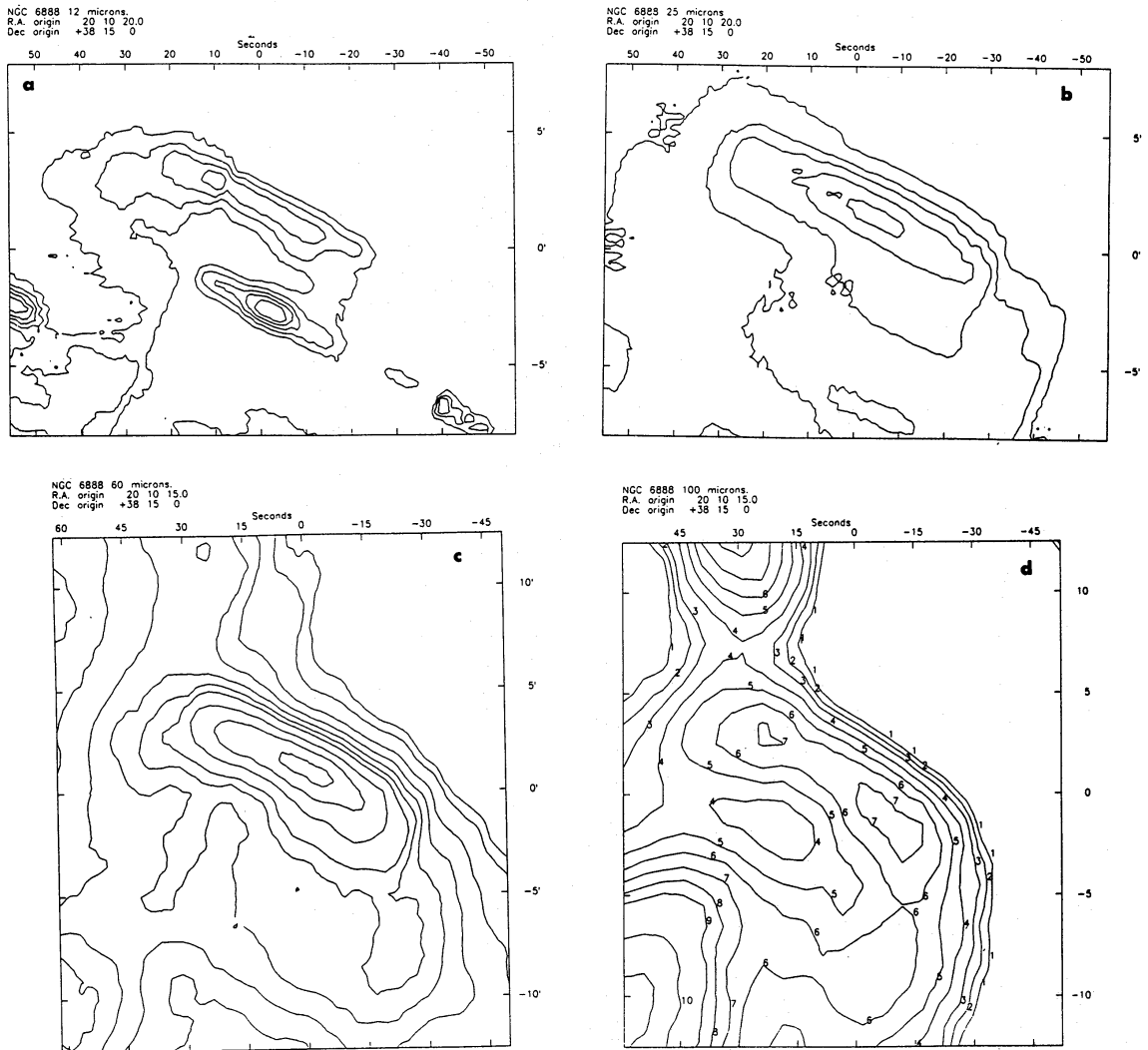


Figure 5. The *IRAS* survey maps (HCON1) of NGC 6888 in 12, 25, 60 and 100 μm wavebands. Contour levels for each are (a) 1, 1.5, 2, 2.5 and 3 MJy/sr (HD192163 appears as a reasonably intense object at the centre of the nebula), (b) 2, 4, 6, 10 and 15 MJy/sr, (c) 3, 5, 10, 15, 20, 25, 30, 40, 50 and 60 MJy/sr, (d) 8(1), 10(2), 12(3), 15(4), 18(5), 21(6), 24(7), 27(8), 30(9), 40(10) and 50(11) MJy/sr.

NGC 6888 from

$$M_{\text{HII}} = 70.2 (I_{\text{H}\alpha} D^2 V_{\text{HII}})^{0.5} M_{\odot} \quad (3)$$

where V_{HII} is the volume of emitting gas which is a fraction (≈ 0.1) of the emitting region. Wendker *et al.* (1975) calculate the emitting gas volume to be 0.4 pc^3 . $I_{\text{H}\alpha}$ is measured in $\text{ergs}^{-1} \text{cm}^{-2}$, D is in parsecs and V_{HII} is in pc^3 for equation (3). This gives an ionized mass of $3.5 \pm 1.2 M_{\odot}$ which compares well with Kwitter's (1981) calculated value of $4.0 M_{\odot}$ at 1.45 kpc.

2.3 *IRAS* MAPS

IRAS maps of the region were produced from survey array (CRDD) data. Scans over a region approximately $50 \times 120 \text{ arcmin}^2$ were obtained of the region surrounding NGC 6888 in all four survey array bands (12, 25, 60 and 100 μm). A two-dimensional quadratic fit was made to the background emission which was then removed from the data arrays. The data obtained are shown as contour maps in Fig. 5, with contour intervals being the signal obtained above sky level.

Table 2. Colour corrected *IRAS* fluxes, luminosity and overall dust temperature for NGC6888.

12 μm	14.1 Jy
25 μm	95 Jy
60 μm	455 Jy
100 μm	439 Jy
$L_{\text{FIR}}(1\text{--}500\ \mu\text{m})$	6.8×10^{36} erg
Dust temp.	33 K

Emission can be seen over the entire nebula and the 100 μm map shows a more complete shell than is observable in visible light. The cool dust is best shown in the 100 μm band where a hole in the emitting area is clearly visible. The warmest part of the dust emission arises in the northern part of the nebula, where the peak in the 25 and 60 μm emission bands are observed. Dust temperatures in the region range from 25 K in the southern part of the nebula to 47 K in the northern half. This compares to dust temperatures in the surrounding medium of ≈ 23 K. It is therefore likely that the grains are collisionally heated in part, although most heating is likely to be from the central WN6 star. The warm material corresponds with the brightest regions of optical line emission observed by Parker (1978) and Johnson & Songsathaporn (1981).

The larger reddening values obtained for knots of emission in NGC 6888 by Parker (1978) are well explained by the extra dust found in the northern part of the nebula. Associated with the excess dust will be extra gas (assuming a roughly constant gas to dust mass ratio across the nebula). The brighter regions of optical line emission are therefore also the regions of highest gas densities. The associated decreases in $H\alpha/[\text{N II}]$ ratios suggest that the optical emission is partially due to collisional ionization by shocks (see Fig. 4). The strong correlation in Fig. 4 between $[\text{N II}]$ line intensity and $H\alpha/[\text{N II}]$ ratio may well be due to excess forbidden line emission from shocks. This couples well with the dynamical information where excess emission is seen to be coming from gas travelling at slightly slower than the normal expansion velocity (see positions A and B on Fig. 2).

It is therefore possible that in these cases a shock is being slowed by a dense region of gas and emitting large amounts of line emission, particularly forbidden lines.

Total fluxes have been estimated from the four intensity maps shown in Fig. 5. These have been colour corrected using the same system as Marston and Dickens (1988). The colour corrected values are listed in Table 2. The luminosity in the far-infrared from 1 to 500 μm is also included in Table 2. All values have associated errors of approximately 10 per cent.

The central Wolf-Rayet star HD192163 was also seen in emission in the 12 μm band with a flux of 0.8 ± 0.1 Jy.

Some of the far-infrared emission may well be associated with emission lines in the nebula (particularly $[\text{O III}]$ 51.8 and 88.3 μm , and $[\text{N III}]$ 57.3 μm in the 60 and 100 μm bands). Indeed Pottasch (1985) noted that between 5 and 30 per cent of planetary nebula far-infrared emission in the *IRAS* 60 and 100 μm bands is due to line emission. Taking the worst case of 30 per cent line emission, the continuum far-infrared fluxes, together with a calculated average temperature for the nebula of 33 K a dust mass of $0.3 \pm 0.1 M_{\odot}$ is suggested. This uses a graphite and silicate mix of grains with 70 per cent of the dust mass in the form of silicate grains. Values for the grain absorption efficiencies were taken from Draine (1981) which gives a frequency dependence to the absorption efficiency of $\approx \nu^2$. The distance to the nebula was taken as 1.45 kpc. It should be noted that the presence of cool dust (< 15 K) mixed in with this warmer dust cannot be ruled out. However, the ambient grain temperature of the region is 23 K, and it is unlikely that large amounts of dust exist below this temperature. The amount of dust formed in WR winds is small

and in the lifetime of HD192163 only $0.004 M_{\odot}$ could have been produced at best (assuming a gas to dust mass ratio of 100), although any grain production is unlikely in the wind of the hot WR star. The dust mass has therefore been swept up into the nebular shell along with the ambient gas. With a gas to dust mass ratio of 100 we arrive at a figure of $30 M_{\odot}$ of swept up material if 30 per cent of the far infrared flux is from line emission. Two conclusions can now be drawn from these arguments:

- (i) approximately 90 per cent of the shell mass in the ring nebula is made of neutral material and
- (ii) the far infrared emission lines of ionized nitrogen and oxygen must therefore contribute little to the observed far-infrared emission as only a small amount of the gas is ionized.

It is more likely that the total dust mass is nearer $0.43 M_{\odot}$ (assuming no line emission) with an associated gas mass of $43 M_{\odot}$. The large amount of neutral material in NGC 6888 is in reasonable agreement with the calculations of Van Buren (1986).

The presence of molecular clouds in the region, seen in the *IRAS* data, may well explain the unusually high value for the density of the ambient medium. This amount of dust produces only a small amount of absorption at visible wavelengths for an even distribution of dust, the optical depth at $H\alpha$ due to dust, τ_D , is given by

$$\tau_D = \frac{3M_D}{16\pi a \rho_D R_s^2} \quad (4)$$

where M_D is the dust mass, a is the radius of the grains absorbing the $H\alpha$ radiation (taken to be 0.1μ), ρ_D is the dust density (taken as 3 g cm^{-3}) and R_s is the radius of the shell (3 pc). This gives a value of τ_D of 0.017.

2.4 FULL-SCALE EVOLUTION

We now have some more accurate figures on the mass and kinematics of NGC 6888, consequently the evolution of the nebula can now be discussed. We shall first make the assumption that NGC 6888 is a pressure driven bubble. Using a mass loss rate for HD192163 of $\dot{M}_W = 2.45 \times 10^{-5} M_{\odot} \text{ yr}^{-1}$ (at 1.45 kpc) together with a terminal velocity of $v_{\infty} = 2250 \text{ km s}^{-1}$ (Barlow, Smith & Willis 1981), the wind luminosity of the WR star is

$$L_W = \frac{1}{2} \dot{M}_W v_{\infty}^2 = 4 \times 10^{37} \text{ erg s}^{-1}. \quad (5)$$

We can now use the adapted equations of Dyson & de Vries (1972) and Weaver *et al.* (1977) formed by Meaburn (1980),

$$L_W = 9.5 \times 10^{17} n_0 V_s^5(t) t^2 \quad (6)$$

and

$$D(t) = 3.5 \times 10^{-6} V_s(t) t. \quad (7)$$

Here, D is the nebular diameter in parsecs, t is the nebular age in years, V_s is the shell expansion velocity in km s^{-1} and n_0 is the ambient gas number density. Using a diameter for the nebula of 6 pc an age for the nebula of $t = 2.0 \pm 0.1 \times 10^4 \text{ yr}$ is obtained. Rearranging equations (5) and (6) an estimate of the ambient density (independent of time-scale) can be found using

$$n_0 = 1.29 \times 10^{-29} \frac{L_W}{V_s^3 D^2} \text{ atom cm}^{-3}. \quad (8)$$

This suggests a value for the ambient density of $n_0 = 23 \text{ atom cm}^{-3}$. The swept up mass from such a density is $\approx 40 M_{\odot}$, with a dependence on the shape of the nebula. This is in close agreement with

the mass estimate made from *IRAS* data and suggests that the shell is mainly composed of swept up ISM or red supergiant ejecta. The abundance enhancements found by Kwitter (1981) for the ionized gas agree well with a mixture containing interstellar material and WR wind material blown off over a period of 2×10^4 yr. It is therefore most likely that the swept up material is mainly ambient ISM, the mass of the shell material being more than would have been ejected by HD192163 in its red supergiant stage of evolution. The total shell mass is much greater than the ionized mass and it is proposed that a neutral shell of gas exists outside the ionized material in the nebula.

The efficiency for the conversion of wind kinetic energy into the kinetic energy of the expanding shell is given by

$$\varepsilon_s = \frac{M_s V_s^2}{\dot{M}_w v_\infty^2 t} \quad (9)$$

and the momentum efficiency is given by

$$\pi_s = \frac{M_s V_s}{\dot{M}_w v_\infty t} \quad (10)$$

Here M_s is the mass of the shell, other parameters are the same as in previous equations. For energy driven bubbles ε_s is predicted to be 0.2 with $\pi_s \gg 1$. In a momentum driven flow predicted values are $\varepsilon_s \ll 1$ and $\pi_s \approx 1$. Values obtained here give a range to ε_s between 0.09 and 0.13 with π_s lying in the range 2.4–3.4, for M_s in the range 30–40 M_\odot . These values strongly suggest that NGC 6888 is an energy conserving expanding bubble rather than momentum conserving as previously put forward by Treffers & Chu (1982).

We therefore have a trapped ionization front, which is ionization bounded where the available rate of Lyman continuum photons (calculated by Van Buren to be 4.7×10^{47} photon s^{-1}) is less than the possible rate of recombinations in the shell. The optical depth in the shell of the nebula is low and little radiation is absorbed by dust. The parameter, i , relates the photon flux to the possible rate of recombinations in the shell and is given by

$$i = \frac{S}{R'} = 3.21 \times 10^4 S_{49} n_s^{-1} m_s^{-1} \mu_H \quad (11)$$

(Van Buren 1986). Where R' is the number of recombinations in the shell, S_{49} is the Lyman photon flux in units of 10^{49} photon s^{-1} , n_s is the number density of particles in the nebular shell, m_s is the shell mass and μ_H is the reduced mass (taken as 1.6). For values of $i > 1$ the shell is completely ionized. For $i < 1$ only a fraction of the shell, given by i , is photoionized. The only value we do not have for this calculation is the number density in the shell. We can use the relation for the balance of ram pressures over a shock to estimate n_s ,

$$n_s = \left(\frac{v_s}{c_s} \right)^2 n_0, \quad (12)$$

here, c_s is the sound speed in the ionized gas, found by Kwitter (1981) to be 12 km s^{-1} (equivalent to an electron temperature of $\approx 8000 \text{ K}$). Our value for i is therefore in the range 0.05–0.07. This is somewhat less than the observed mass fraction of ionized gas (0.09) and suggests that some gas in the nebula may well be collisionally ionized.

2.5 THE SHAPE OF NGC 6888

The shape and motions within the nebula are governed by the external medium. The ambient density is not uniform, however, and a number of patches of emission are observed in the echelle

observations to have lower velocities than the expansion velocity. This suggests that the nebula is entering regions with gas densities that are higher by a factor $(V_s/V_{LV})^2$, where V_{LV} is the observed velocity of the emitting material. For the region marked B on Fig. 2 this implies a particle density of 30 atom cm^{-3} , while in the region marked A ambient densities may well be as high as 100 atom cm^{-3} . Material moving with higher velocities than the expanding ellipse are probably associated with regions of lower ambient density than 23 atom cm^{-3} .

3 Conclusions

The ring nebulae surrounding WR stars, such as NGC 6888, have presented several theoretical problems. This has been mainly due to the apparent lack of mass associated with them. Results presented here have shown the first observational evidence for a shell of swept up neutral material in addition to the ionized shell of NGC 6888. A similar shell has been detected around θ Muscae by Cappa de Nicolau & Niemela (1984). Several conclusions from our results can be made regarding the origin and evolution of the nebula.

(1) The dust associated with the nebula has been swept up from the surrounding medium and has an associated gas mass of $30\text{--}43 M_{\odot}$. This is much larger than the ionized gas mass of $\approx 3.5 M_{\odot}$ assuming a gas to dust ratio of 100.

(2) Optical line profiles along the major axis of the nebula reveal a bubble of material expanding at $85 \pm 3 \text{ km s}^{-1}$ with a radius of 3 pc.

(3) The larger shell mass obtained suggests that energy conservation exists within the nebula when comparing energy and momentum efficiencies, assuming the expansion is driven by the wind of the central WR star.

(4) Using the kinematical information obtained from the echelle data, an energy conserving model (Dyson & de Vries 1972; Weaver *et al.* 1977) can be used which also fits the *IRAS* data giving an ambient density of $\approx 23 \text{ atoms cm}^{-3}$.

(5) The nebular shell is found to be ionization bounded, from the point of view of the radiative ionization caused by the central star. In other words, the calculated ionizing flux of Lyman photons suggests that only an inward facing fraction of the neutral shell is photoionized. There may, however, be a thin outer zone to the neutral shell, of shock ionized gas produced as the ambient ISM passes through the outer shock caused by the nebular expansion. This is indicated by the excess of the turbulent widths of the [N II] line profiles over those of $H\alpha$ which suggests more than one emitting region.

(6) Deviations in the observed motions of the shell may be explained by the expanding shell colliding with regions of higher particle density, with regions of up to $100 \text{ atoms cm}^{-3}$. This may be explained by the presence of cool molecular clouds in the region observed in the *IRAS* data.

(7) Most of the area of ionized gas in the nebula, has been ionized by the central WR star, however, regions of low $H\alpha$ /[N II] ratio exist, together with warm dust, in patches across the nebula. Kwitter (1981) has noted no obvious variation in abundances across the nebula, so these regions are believed to be caused by collisional ionization. As the ionized fraction is slightly higher than predicted in Section 2.5, it is believed that some of the nebula is also collisionally ionized. These regions with low $H\alpha$ /[N II] ratios also have higher ambient densities with warm dust, heated by the excess UV from the shock front, and low $H\alpha$ /[N II] ratios due to the collisional ionization. These regions are also characterized by lower expansion velocities, as mentioned in (6).

(8) The central component of the three components observed in the nebula (at $V_{\text{LSR}} = 12 \text{ km s}^{-1}$) must come from ionized material along the line of sight but external to NGC 6888, created by hot OB stars. A likely candidate for this ionizing radiation is the Cygnus OB1 association. The neighbouring regions of molecular clouds, containing young stars, may well be the source for this

background radiation. A halo of emission to NGC 6888 is ruled out as all the ionizing flux is absorbed in the nebula.

(9) Warm dust, associated with regions of high gas density, has most likely been heated collisionally, something that has been noted previously in supernova remnants (see e.g. Braun & Strom 1986a, b).

(10) No peculiar bowshock motions or knots of high nitrogen abundance are noted in NGC 6888 (as compared to RCW 104).

The overall situation reveals NGC 6888 as a pressure driven bubble expanding into a dense, inhomogeneous ambient medium. This has given rise to collisional as well as radiative ionization in the shell and collisional heating of dust grains swept up from the ambient medium. The majority of the shell material must be from the interstellar medium as the implied shell mass is too high to be simply red supergiant ejecta of the outer shell of the WR star. However, at least part of the inner ionized component of the nebula has its source in material from the WR wind (Kwitter 1981) and the present results do not preclude the existence of red supergiant or WR ejecta material existing in the shell together with ISM. Although there is good agreement between the dynamical mass of the shell and that of swept up ISM from dust masses, the gas to dust ratio needs to be only slightly lower for several solar masses of stellar ejecta to also exist in the shell.

It would be interesting to attempt the detection of neutral shells of material around WR stars using 21 cm and $2.2\ \mu\text{m}$ (molecular hydrogen line) measurements indicating the presence of both atomic and molecular hydrogen. The hydrogen column density predicted for the shell of NGC 6888 being $\approx 8 \times 10^{19}\ \text{cm}^{-2}$ (Van Buren 1986). Nebulae such as NGC 2359, RCW 104 and NGC 7635, also associated with Wolf–Rayet stars, are calculated to have column densities twice as large.

The possibility remains that the far infrared emission from the shell around NGC 6888 reported here, consists almost entirely of emission lines, in which case the present estimation of the total expanding mass of NGC 6888 is far too high. Far-infrared spectra are needed to confirm that continuum from warm dust dominates the emission.

Acknowledgments

We wish to thank the staff of the Isaac Newton Telescope for help during our observing run in 1987 July. We are also grateful to Dave Axon and Tim Wilkins for use of their LONGSLIT program in the reduction of these data.

Note added in proof

Van Buren & McCray (1988, *Astrophys. J.*, **329**, L93) have just concluded that the emissions from NGC 6888 in the *IRAS* 60 and $100\ \mu\text{m}$ bands are predominantly from the [O III] lines, in which case the neutral mass would be negligible. However, an estimation of the [O III] infrared line fluxes from measurements of the [O III] 5007 Å flux and interstellar extinction ($c=1.25$) suggests that this is only marginally possible. Far-infrared spectra in these two bands are awaited to decide the issue conclusively. It should also be noted that Whittet *et al.* (1979, *Mon. Not. R. astr. Soc.*, **189**, 519) find a violet-displaced component in the Na I interstellar absorption line profiles in the light of the Wolf–Rayet star in the centre of NGC 6888. A co-expanding neutral shell, as proposed in the present paper, is suggested.

References

- Barlow, M., Smith, L. J. & Willis, A. J., 1981. *Mon. Not. R. astr. Soc.*, **196**, 101.
 Boksenberg, A. & Burgess, D. E., 1973. *Proc. Symp. TV Sensors*, p. 21, Vancouver.

- Braun, R. & Strom, R. G., 1986a. *Astr. Astrophys.*, **164**, 193.
Braun, R. & Strom, R. G., 1986b. *Astr. Astrophys.*, **164**, 208.
Cappa de Nicolau C. & Niemela, V. S., 1984. *Astr. J.*, **89**, 1398.
Conti, P. S., Garmany Catharine D., de Loore C. & Vanbeveren, D., 1983. *Astrophys. J.*, **274**, 302.
Draine, B. T., 1981. *Astrophys. J.*, **245**, 880.
Dyson, J. E. & de Vries, J., 1972. *Astr. Astrophys.*, **20**, 233.
Goudis, C. Meaburn, J. & Whitehead, M., 1988. *Astr. Astrophys.*, **191**, 341.
Hartquist, T. W., Dyson, J. E., Pettini, M. & Smith, L. J., 1986. *Mon. Not. R. astr. Soc.*, **221**, 715.
Johnson, H. M. & Hogg, D. E., 1965. *Astrophys. J.*, **142**, 1033.
Johnson, P. G. & Songsathaporn, R., 1981. *Mon. Not. R. astr. Soc.*, **195**, 51.
Kwitter, K. B., 1981. *Astrophys. J.*, **245**, 154.
Lozinskaya, T. A., 1970. *Soviet Astr. A. J.*, **14**, 98.
Marston, A. P. & Dickens, R. J., 1988. *Astr. Astrophys.*, **193**, 27.
Meaburn, J., 1980. *Mon. Not. R. astr. Soc.*, **192**, 365.
Meaburn, J., 1983. *Astr. Astrophys.*, **122**, 111.
Meaburn, J., Blundell, B., Carling, R., Gregory, D. F., Keir, D. & Wynne, C., 1984. *Mon. Not. R. astr. Soc.*, **210**, 463.
Parker, R. A., 1978. *Astrophys. J.*, **224**, 873.
Pottasch, S. RE., 1985. *Workshop on Model Nebulae*, p. 89, ed. D. Pequinot, Observatoire de Meudon.
Stone Remington, P. S., 1974. *Astrophys. J.*, **193**, 135.
Treffers, R. R. & Chu You-Hua, 1982. *Astrophys. J.*, **254**, 569.
Van Buren, D., 1986. *Astrophys. J.*, **306**, 538.
Weaver, R., McCray, R., Castor, J., Shapiro, P. & Moore, R., 1977. *Astrophys. J.*, **218**, 377.
Wendker, H. J., Smith, L. F., Isrel, F. P., Habing, H. J. & Dickel, H. R., 1975. *Astr. Astrophys.*, **42**, 173.